Numerical aspects of using vertical equilibrium models for simulating CO2 sequestration

I. Ligaarden, H. M. Nilsen

August 16, 2010

Abstract

Storage of CO2 in deep saline aquifers is considered an important means to reduce anthropogenic CO2 in the atmosphere. Assessing the risk of storage operations requires accurate modeling of migration of injected CO2. However, since potential injection sites typically are very large and time-scales long, flow simulation with traditional methods from the petroleum industry is often not feasible. Also, CO2 is very mobile and the flow is usually confined to thin layers, which put severe requirements on the vertical grid resolution.

Using a vertical equilibrium assumption, the flow of a layer of CO2 can be approximated in terms of its thickness to obtain a 2D simulation model. Although this approach reduces the dimension of the model, important information of the heterogeneities in the underlying 3D medium is preserved.

In this paper, we consider the Johansen formation, a candidate for CO2 sequestration, to compare the use of 3D simulations to simulations with a vertical equilibrium 2D model. We discuss numerical aspects of using the different methods, and demonstrate that the vertical equilibrium model provides more accurate results when the vertical grid resolution is low. Moreover, we investigate how averaging of parameters influences the accuracy of the vertically equilibrium solution.

Introduction

Climate change due to anthropogenic CO_2 emissions is believed to be a major treat to the global climate (Metz et al., 2005). The worlds energy consumption is likely to increase in the future, and with that the need to to utilize the remaining worlds fossil fuel resources. Large scale project with CO_2 capture and subsequent storage (CCS), is a promising technology for reducing emissions to the atmosphere. If CCS should become a viable option, large thorough investigations of the risk of leakage from the chosen storage sights are necessary. Due to large uncertainties in geology, multiple simulations would be required for risk analysis. This creates a need for fast simulation tools particularly tuned for the situation of CO_2 injection and subsequent CO_2 migration.

One promising candidate for fast and accurate modeling of CO_2 sequestration is based on the vertical equilibrium (VE) assumption. VE models have a long tradition for describing flow in porous media; in hydrology it is known as the Dupuit approximation, whereas in the oil industry, VE models were early on extended to simulate two-phase and three-phase segregated flow (Martin, 1958; Coats et al., 1967; Martin, 1968). In particular, Coats et al. (1971) advocated comparing simulations of 2D vertical cross-sections to corresponding 1D simulations with a vertical averaged model to check if the assumptions for the latter were present, and then use this model to save computational time or gain resolution whenever applicable. But as computational resources increased, VE models became less and less used. However, for situations with strong gravity segregation (like steam injection) interface models have been an active research area (Godderij et al., 1999; Neuman, 1985).

Recently, there has been a renewed interest in VE methods as a means to simulate large-scale CO_2 migration, for which a sharp-interface assumption with vertical equilibrium may be reasonable due to
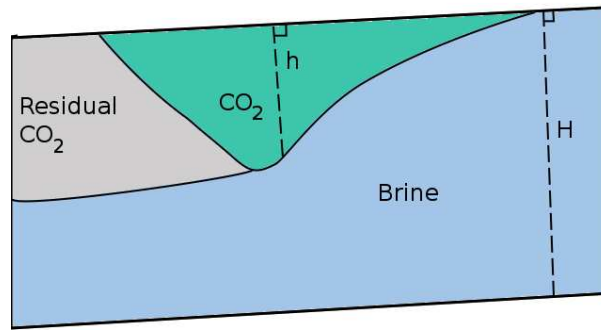
***Figure 1** Illustration of the CO$_2$ plume as assumed in the VE modeling.*

the large density differences between super-critical CO$_2$ and brine (see e.g. Nordbotten et al. (2005); Celia et al. (2006); Nordbotten and Celia (2006)). Indeed, in many cases the errors resulting from the VE assumption may be significantly less that the errors introduced by the overly coarse resolution needed to make the 3D simulation model computationally tractable. Vertical equilibrium simulations may then be attractive to increase (lateral) resolution while saving computational cost.

The VE formulation for multiphase flow in heterogeneous media leads to a system of a pressure equation and a transport equation that can be written in a standard fractional-flow formulation. Many authors (Hesse et al., 2007, 2008; MacMinn and Juanes, 2009; Huppert and Woods, 1995; Lyle et al., 2005; Vella and Huppert, 1995) have considered gravity-driven flow in the VE equations in detail. Most of this work has concentrated on analytical aspects and simplified geometry. In the benchmark study by Class et al. (2009), calculations using the VE equations compared well with 3D simulations. This work was continued in (Gasda et al., 2009), where VE equations were used together with sub-scale analytic functions to show the potential of using the VE model to speed up calculations of simulating CO$_2$ sequestration.

Herein we focus on studying the validity of the VE model in time and space for a realistic CO$_2$ injection scenario. In the same domains we study the shortcoming of 3D simulation to accurately incorporate sharp interfaces without special modification. We consider how the magnitude of different terms in the 3D simulation and VE simulation impacts the choice of numerical method. In particular, we point out how the vertical equilibrium formulation change the requirements for the pressure saturation splitting step. Moreover, we perform both 3D and VE simulations on the Johansen formation to show that the grid resolution also is an important factor for the applicability of the numerical methods. The difference between the injection period and post injection period will be discussed in this context. Furthermore, a VE model can be made using different approximations for the porosity and permeability of the 3D model, and we investigate the impact of these simplifications on the accuracy of the simulation result.

Mathematical model

In this paper we consider immiscible incompressible flow, which is a strict approximation. These simplifications make the comparison of terms for the 3D and VE formulation more transparent. Moreover, the presentation of how to avoid pitfalls in order to obtain accurate simulation results becomes clearer.

We start with the two mass conservation equations for incompressible flow without capillary forces for the phase pressure p_i, velocity $\mathbf{v}_i$, and saturation S_i for each phase i = {CO$_2$, water}, given at the spatial coordinate $\mathbf{r}$,

$$\frac{\partial \phi(\mathbf{r}) S_i}{\partial t} + \nabla \cdot \mathbf{v}_i = q_i, \qquad \mathbf{v}_i = -\lambda_i(S) K(\mathbf{r})(\nabla p_i - \rho_i \mathbf{g}). \tag{1}$$

Here ϕ, K, ρ_i, μ_i, $k_i(S)$, and q_i denotes the porosity, permeability, density, viscosity, relative permeability function, and volume rate of source, respectively. Further, the mobility is $\lambda_i(S) = k_i(S)/\mu_i$.

The above equations can be reformulated in a pressure and saturation equation by defining a global pressure p and the total velocity $\mathbf{v}$,

$$\frac{\partial \phi(\mathbf{r})S}{\partial t} + \nabla \cdot f(S)\Big[\mathbf{v} + \lambda_w(S)K\Delta\rho\mathbf{g}\Big] = q_{co_2},$$

$$\mathbf{v} = -K\lambda_t\Big[\nabla p - \big(f(S)\rho_{co2} + [1-f(S)]\rho_w\big)\mathbf{g}\Big], \quad \nabla \cdot \mathbf{v} = q_{\text{tot}}, \tag{2}$$

where $\lambda_t(S) = \lambda_{co2}(S) + \lambda_w(S)$, $f(S) = \lambda_{co2}(S)/\lambda_t(S)$, $\Delta\rho = \rho_{co2} - \rho_w$ and S is the saturation of CO_2. The above equations are vertically averaged to obtain a vertical equilibrium model. Herein we only present the equations, and refer the reader to one of Martin (1958); Coats et al. (1967); Martin (1968) for a thorough derivation of vertical equilibrium models. Since capillary pressure is neglected in our model, the result is a sharp interface approximation. We define the averaged saturation $s = h/H$ to be the relative height of the CO_2 plume, such that s is a function of time t and the spatial position $\mathbf{x}$ along the dipping reservoir, see Figure 1. This yields the following equations,

$$\frac{\partial \Phi(s, \mathbf{x})}{\partial t} + \nabla_\| \cdot \Big[\tilde{f}(s, \mathbf{x})\mathbf{v}^{ve} + \tilde{f}_g(s, \mathbf{x})\big(\mathbf{g}_\|(\mathbf{x}) + \nabla p_c(s, \mathbf{x})\big)\Big] = q_{co2}(\mathbf{x}),$$

$$\nabla_\| \cdot \mathbf{v}^{ve} = q_{tot}(\mathbf{x}), \tag{3}$$

$$\mathbf{v}^{ve} = -\tilde{\lambda}_t(s, \mathbf{x})\Big[\nabla_\| p_t - \big(\tilde{f}(s, \mathbf{x})\rho_{co2} + [1 - \tilde{f}(s, \mathbf{x})]\rho_w\big)\mathbf{g}_\|(\mathbf{x}) + \frac{\tilde{\lambda}_w(s, \mathbf{x})}{\tilde{\lambda}_t(s, \mathbf{x})}\nabla_\| p_c(s, \mathbf{x})\Big],$$

where $\|$ means parallel to the surface and $p_t(\mathbf{x})$ is the pressure at the top surface. The function $\Phi(s, \mathbf{x})$ is the integrated porosity,

$$\Phi(s, \mathbf{x}) = \int_0^{H(x)s} \phi(z, \mathbf{x})dz, \tag{4}$$

that is a nonlinear function of the averaged saturation s. If the porosity is constant in the vertical direction, the above expression reduces to $\Phi(s, \mathbf{x}) = \phi(\mathbf{x}) \cdot sH(\mathbf{x})$. Moreover, the function $\mathbf{g}_\|$ is the gravity component along the surface, $\mathbf{v}^{ve}$ is the integral of the velocity in the aquifer, and q the source term. When we disregard capillary forces in the underlying flow model, our VE-equivalent of the capillary term reads $p_c(s, \mathbf{x}) = H(\mathbf{x})g_\perp\Delta\rho\,s$, where $g_\perp$ is the gravity component perpendicular to the surface. Lastly, the heterogeneities in the underlying 3D medium is preserved through the spatially dependent pseudo mobilities and fractional flow functions given by

$$\tilde{\lambda}_{co_2}(s, \mathbf{x}) = \int_0^{sH(\mathbf{x})} \frac{k_{co_2}(1)}{\mu_{co2}}K_\|(z, \mathbf{x})dz, \qquad \tilde{\lambda}_w(s, \mathbf{x}) = \int_{sH(\mathbf{x})}^{H(\mathbf{x})} \frac{k_w(1)}{\mu_w}K_\|(z, \mathbf{x})dz,$$

$$\tilde{f}(s, \mathbf{x}) = \frac{\tilde{\lambda}_{co_2}(s, \mathbf{x})}{\tilde{\lambda}_{co_2}(s, \mathbf{x}) + \tilde{\lambda}_w(s, \mathbf{x})}, \qquad \tilde{f}_g(s, \mathbf{x}) = \tilde{\lambda}_w(s, \mathbf{x})\tilde{f}(s, \mathbf{x}), \tag{5}$$

where k_α denotes the relative permeabilities of brine and CO_2. When residual trapping is considered, the evaluation of the relative permeabilities includes the residual saturations given as S_{rw} and S_{rco2} for brine and CO_2 respectively. Then k_{co2} is evaluated in $1 - S_{rw}$ everywhere, while k_w is evaluated in $1 - S_{rco2}$ where the historical maximum of the average saturation is larger than the current averaged saturation, $s_{max} > s$. Moreover, $\Phi(s, \mathbf{x})$ is also multiplied by $1 - (S_{rw} + S_{rco_2})$ where $s_{max} > s$ and with $1 - S_w$ elsewhere.

One simplification to the above model is to use permeability and porosity that is averaged in the vertical direction. The resulting pseudo mobilities are then given by

$$\tilde{\lambda}_{co_2,avg}(s, \mathbf{x}) = \frac{k_{co_2}(1)}{\mu_{co2}}s\int_0^{H(\mathbf{x})} K_\|(z, \mathbf{x})dz, \qquad \tilde{\lambda}_{w,avg}(s, \mathbf{x}) = \frac{k_w(1)}{\mu_w}(1 - s)\int_0^{H(\mathbf{x})} K_\|(z, \mathbf{x})dz,$$

$$\tag{6}$$
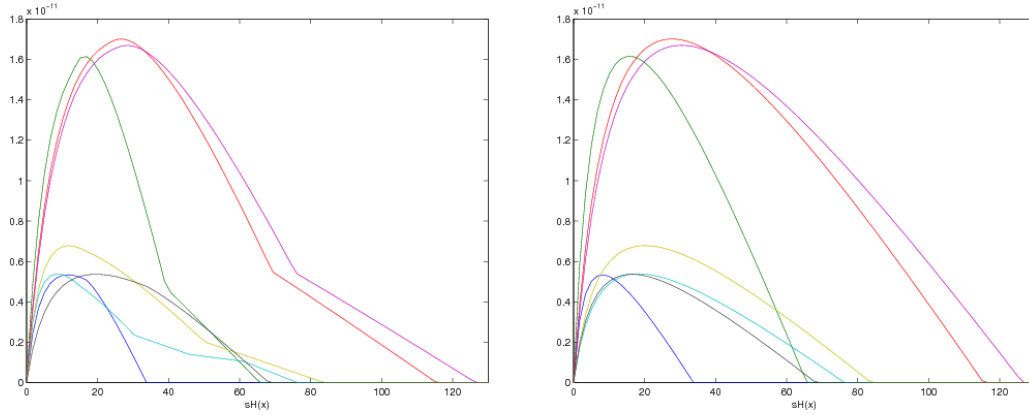
Figure 2 *Selection of pseudo mobility functions from the Johansen formation. Left: vertically integrated pseudo mobility functions (Eq.* (5)*). Right: averaged pseudo mobility functions (Eq.*(6)*).*

and the transport equation take the simpler form

$$\phi_{avg}(\mathbf{x})\frac{H(\mathbf{x})\partial s}{\partial t} + \nabla \cdot \left[\tilde{f}_{avg}(s,\mathbf{x})\mathbf{v}^{ve} + \tilde{f}_{g,avg}(s,\mathbf{x})\left[\mathbf{g}_\|(\mathbf{x}) + \nabla p_c(s,\mathbf{x})\right]\right] = q_{co_2}(\mathbf{x}). \qquad (7)$$

This approximation may give good results if the permeability field varies little in the vertical direction, but becomes a coarse approximation with large variations. In particular, for a CO_2 injection scenario the permeability on the top of the reservoir is most important. We will compare the result of using averaged permeability and porosity (Eq. 7 versus using the full model (Eq. 3 and Eq. 5)) on the Johansen formation later on. A display of selected pseudo mobility curves from Johansen is shown in Figure 2.

To analyze the strength of the different terms in the two-phase flow equations and how they differ between the VE formulation and the 3D simulation, we first decompose the total velocity of the 3D equation into two parts $\mathbf{v}_{adv}$, and $\mathbf{v}_{conv}$, which we call advection and convection, respectively. They correspond to the solution of the elliptic equations

$$\begin{aligned}
\nabla \cdot \mathbf{v}_{adv} &= q, \qquad \mathbf{v}_{adv} = -K\lambda_t(S)\nabla p_{adv}, \\
\nabla \cdot \mathbf{v}_{conv} &= 0, \qquad \mathbf{v}_{conv} = -K\lambda_t(S)(\nabla p_{conv} - (f(S)\rho_{co_2} + (1 - f(S))\rho_w \mathbf{g}).
\end{aligned} \qquad (8)$$

This decomposition of the vector field $(\lambda_t K)^{-1}\mathbf{v}$ into an irrotational and a solenoidal vector field will be used to analyze the time step restrictions for the model later on. The corresponding terms in the vertical equilibrium formulation are

$$\begin{aligned}
\nabla_\| \cdot \mathbf{v}_{adv}^{ve} &= q, \qquad \mathbf{v}_{adv} = -\tilde{\lambda}_t^{ve}(s,\mathbf{x})\nabla p_{t,adv}, \\
\nabla_\| \cdot \mathbf{v}_{conv}^{ve} &= 0, \\
\mathbf{v}_{conv}^{ve} &= -\tilde{\lambda}_t(s,\mathbf{x})\left[\nabla_\| p_{t,conv} - \left(\tilde{f}(s,\mathbf{x})\rho_{co2} + (1 - \tilde{f}(s,\mathbf{x}))\rho_w\right)\mathbf{g}_\|(\mathbf{x}) + \frac{\tilde{\lambda}_w(s,\mathbf{x})}{\tilde{\lambda}_t(s,\mathbf{x})}\nabla_\| p_c(s,\mathbf{x})\right].
\end{aligned} \qquad (9)$$

The velocity field $\mathbf{v}_{conv}$ from the 3D equations is here decomposed into to parts, mainly: $\mathbf{v}_{conv}^{ve}$ and a second part that is integrated into the hyperbolic and parabolic terms of the transport equation in the VE formulation. This reduces the coupling between the pressure and transport equation significantly for our problem, which is beneficial as it enables use of longer pressure time steps.

The velocity generated by gravity in the VE model, $\mathbf{v}_{conv}^{ve}$, can be seen to depend on the change in the vertical coordinate of the surface perpendicular to the tilt direction of the interface between CO_2 and brine (i.e. for a 3D case with coordinates (x,y,z) where the interface is tilted in the x-direction, $\mathbf{v}_{conv}^{ve}$ will depend on $\nabla_y z$). Streamlines of this velocity field on the Johansen formation is shown in Figure 3 after 100 years of simulation. The figure also shows the streamlines from $\mathbf{g}_\|(\mathbf{x})$ that corresponds to the part of the 3D vector field $\mathbf{v}_{conv}$ that is integrated into the hyperbolic part of the VE transport equation.
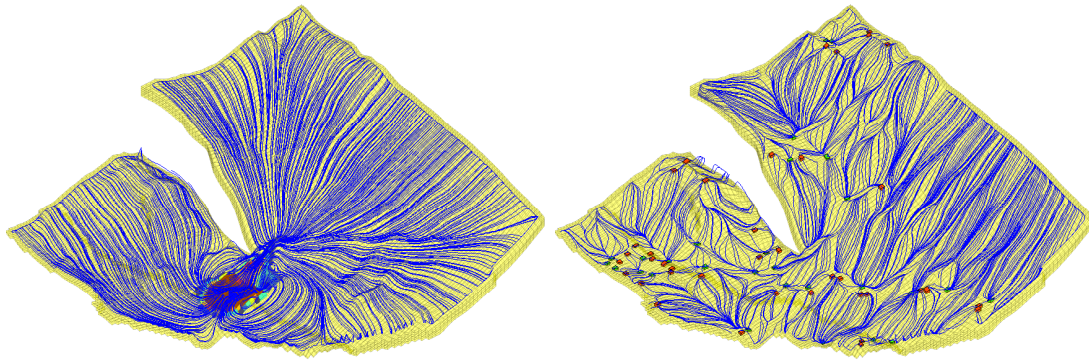
Figure 3 *The left figure is the streamlines of $\mathbf{v}_{conv}^{ve}$ after 100 years of simulation on Johansen. The right figure shows gravity lines of the top surface, where the cells that correspond to local maxima of the surface are colored red and cells that correspond to local minima are colored green.*

Numerical examples

Several formations have been identified as candidates for long term CO_2 storage. We base our numerical examples on one of them, the Johansen formation, a deep saline aquifer in the North sea which is considered to be used for storage in a future pilot project for CCS at Mongstad, Norway. The model has been studied recently by several authors (Eigestad et al., 2009; Bergmo et al., 2009), and is available online (see Eigestad et al. (2008)). Herein we consider a sector model NPD5 of Johansen consisting of the lower three geological zones. This model was used for simulations in Eigestad et al. (2009), and the analysis showed that a rather fine resolution is needed in the vertical direction to accurately describe how a CO_2 plume moves along the top of the formation in the model. The same observation was made by Lingli and Fredrik (2009). This clearly motivates the use of vertical equilibrium methods where the resolution in the vertical direction is not an issue.

The purpose of using vertical equilibrium models is to be able to do fast simulations on large scale potential storage sites like the Johansen formation. So far most VE models for CO_2 storage have been applied to simple models. Benchmark studies involving vertical equilibrium techniques have been applied to an idealized upscaled/sub-model of Johansen in (Class et al., 2009). In this idealized model the grid has simplified geometry and is a fraction of the size of the real Johansen formation. Moreover the permeability and porosity used in this benchmark study is a simplified smoothed version of what is supplied in (Eigestad et al., 2009). In (Gasda et al., 2009), the full Johansen formation is simulated with a vertical equilibrium model using an IMPES strategy.

In this work we take a different approach and investigate features of VE models and 3D models to determine which numerical methods are applicable for simulating CO_2 injection on Johansen. For this purpose we use two different models. First we use a 2D cut of a part of the Johansen formation, visualized in Figure 4, to compare the accuracy of VE and 3D simulations. Subsequently, VE simulations are run on the full NPD5 sector model of Johansen to compare how averaging of parameters influences the accuracy of the VE solution. We use a similar simulation setup to what was done in Eigestad et al. (2009), wherein the model is rigorously described. Therefore, only a short description of the model is provided herein.

The sector model is covered with shales that are thick above the top and bottom, with a permeability of 0.01 mD and 0.1 mD, respectively. Since the flow in these layers is assumed to be negligible, they are replaced by no-flow boundaries in the simulation model. The remaining model has a heterogeneous permeability field that ranges from 5 to 875 mD, and the porosity varies from 10% to 30%. Furthermore, the main fault, easily seen in Figure 5, is assumed to be sealing since the top layers of the sector model
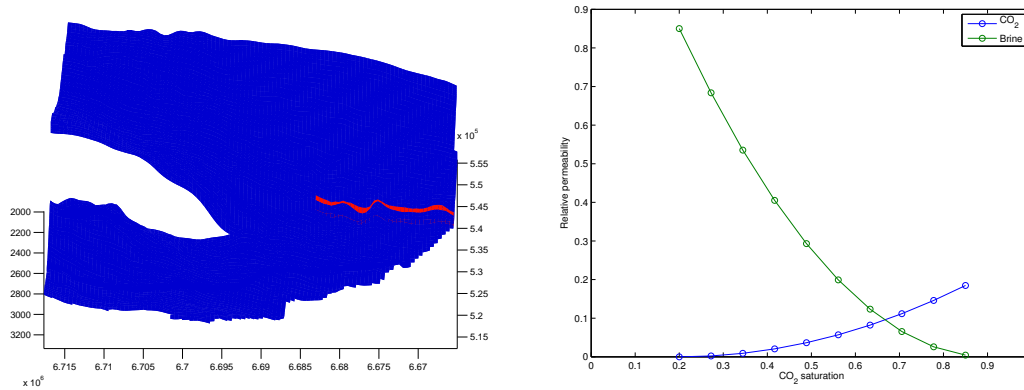
Figure 4 *Right: The different simulation models used in the numerical study; full model in blue and the 2D model in red. Left: Relative permeability curves for CO_2 and brine.*
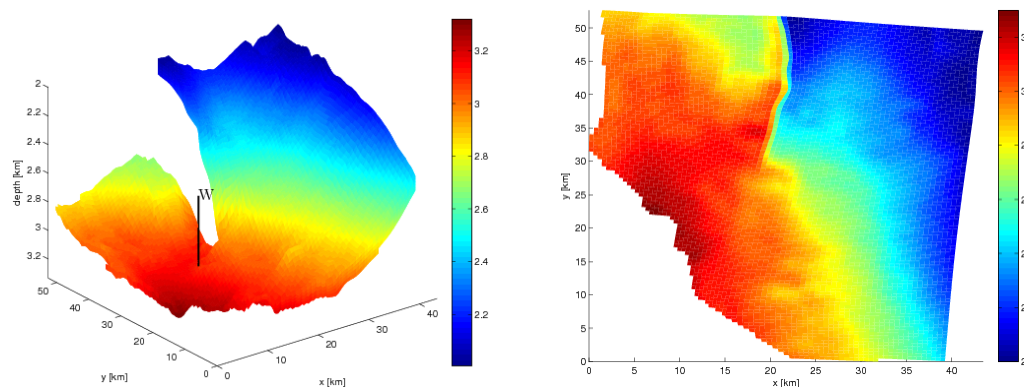

Figure 5 *The left plot shows a height-map of the Johansen sector model with the well indicated. The right plot shows the z-coordinates of the cells in the corresponding 2D grid used in the vertical equilibrium simulation (here the main fault is modeled as an internal no-flow boundary).*

has a high clay/silt content, and the fault is therefore applied with no-flow boundary conditions. The formation is assumed to be at hydrostatic equilibrium when injection of CO_2 starts, thus the remaining boundaries are prescribed hydrostatic pressure boundary conditions.

For both simulation models we use a fluid model similar to what is used in several benchmark studies for CO_2 injection Class et al. (2009); Dahle et al. (2009) and in the specific study on Johansen (Eigestad et al., 2009). The fluid properties are reference values for CO_2 and brine taken at 300 bar. At this pressure, the approximative viscosity and density of supercritical CO_2 is 0.057 cP and 686.54 kg/m^3, respectively, while for brine the viscosity and density is 0.30860 cP and 975.86 kg/m^3. The relative permeability curves are displayed in Figure 4. As can be seen from the figure, residual trapping is accounted for by setting the residual saturation of CO_2, $S_{rco_2} = 0.2$, and for brine, $S_{rw} = 0.1$.

Case 1 (2D cut of Johansen) *We start by considering the 2D cut shown in Figure 4. The purpose of this model is to investigate the accuracy of the 3D and 2D simulation framework. In particular we focus on the vertical resolution of the 3D model. The setup is taken as a vertical slice from the Johansen formation that is sightly simplified to obtain the 2D grid shown in Figure 6. We vary the z-resolution for the 3D simulator from 5 cells, the same as the original Johansen, to 20 cells, which is what was used in Eigestad et al. (2009). For simplicity we disregard residual trapping and use endpoints equal to 1 for the relative permeability curves. The permeability is set to 200 mD and the porosity to 20%.*

In this case we focus on the post injection dynamics, or equivalent the behavior of the plume far from the injector. We use no-flow boundary conditions and an initial plume placed in a stratigraphic trapping
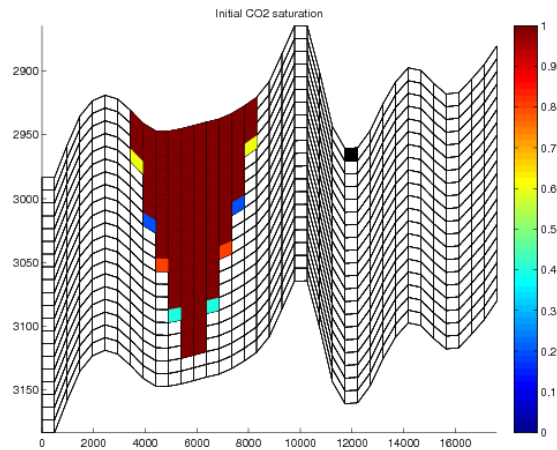
Figure 6 *Plot of 2D model showing initial CO_2 saturation. The spill point is marked with black color.*

region, but with a size which is somewhat to large for the trap, see Figure 6. The distribution of CO_2 after 2000 years for the VE formulation and several 3D models with different vertical resolutions is shown in Figure 7. We see that the 3D simulations require a very fine z resolution to get correct flux over the spill point. The figures also show the relative error in the volume of CO_2 beyond the spill point for the 3D models compared to the VE simulation. We remark that the differences were larger at earlier time steps, which we attribute to the inability of the 3D model to capture the correct flow of thin layers at the top of the formation. Moreover, we did calculations using linear flux functions. For the coarsest 3D model with z-resolution of 5 cells, the relative volume error decreased from 0.74 to 0.14.

This example illustrate the danger of using a nonlinear model (e.g. flux function) on a coarse grid. In this simulation the main contribution to differences was the averaging of $f(s)$ in the transport equation (2). Indeed, when performing large scale simulations, there are two sensitivities that make accurate results hard to obtain, mainly; the sensitivity to grid refinement and the sensitivity of the result to the relative permeability curves.

Case 2 (Full Johansen) *To relate our observation to a full realistic CO_2 storage site, we now simulate on the full Johansen formation. The injection scenario consist of 110 year of injecting 3.5 Mt CO_2 per year and a we simulate 400 years of post injection. The well is placed at the coordinates $(55\ 55\ 6)$. The well placement and the 2D grid used in the VE simulation are displayed in Figure 5.*

In this case we only use the quite coarse original 3D grid, where the typical grid cell size is $500 \times 500 \times 20m$. We do not expect this result to be quantitatively correct, but it gives the right scaling of the different dynamical processes. Through the study of these processes, we can evaluate the applicability of specialized numerical methods for the CO_2 injection problem. Even with this very coarse vertical grid resolution, the qualitative behavior is correct where the upper grid cell is largely filled. As seen in the previous example, the VE model has a much larger extension of the region with a thin CO_2 layer. It is in this region where the Dupuit assumptions of the VE formulation is best fulfilled as seen in Figure 8.

For the VE model we compare the results obtained by using vertically averaged permeability values with the results from using nonlinear pseudo mobility curves (defined in Eq. 5). The differences between the pseudo mobility curves for the two approaches are illustrated in Figure 2. The results in Figure 9 show that the calculations using average permeabilities make the flow go to slow along the upper surface. This is because the permeability of Johansen in general increases towards the top. Consequently, the averaging of the permeability leads to an underestimation of the flow where the layer of CO_2 is thin relative to the height of the formation. Figure 10 shows a 2D cut in the x-direction including the well. The low permeability in the lower layers to the right of the well explains the largest differences between
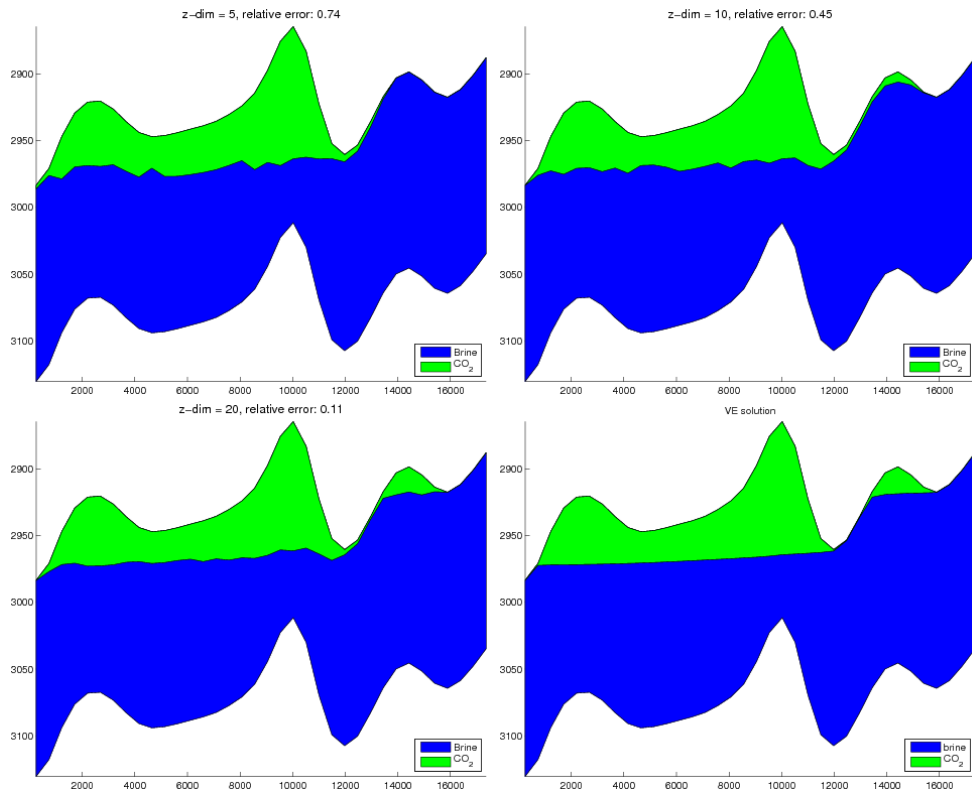
Figure 7 *CO_2 distribution after 2000 years of simulation computed with 3D simulator for different z-resolutions and for vertical equilibrium model (bottom right). A rather fine z-resolution is needed to get accurate results for the 3D simulator.*
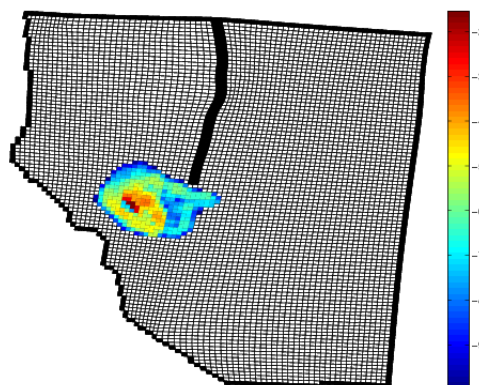
Figure 8 *The Dupuit approximation (vertical equilibrium) is valid if $\omega = K_x/K_z(dh/dx)^2 << 1$. Here $\log(\omega)$ is plotted at the time of end of injection. The approximation is valid except very close to the well.*
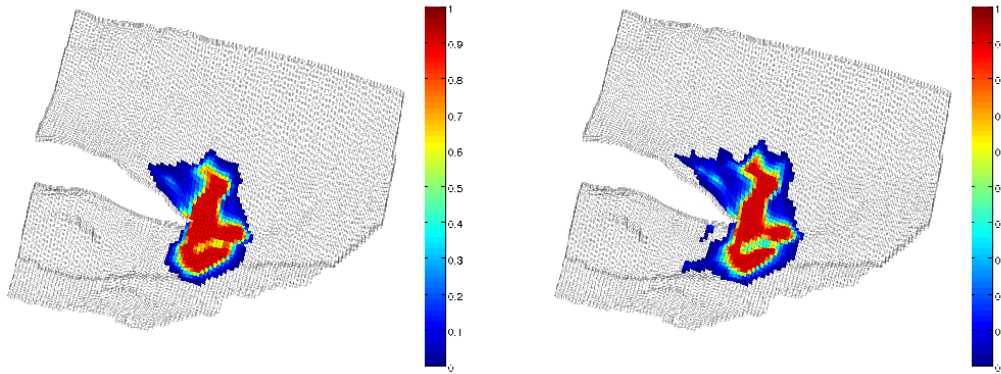
Figure 9 *CO$_2$ saturation for VE simulation with averaged permeability (left) and VE with nonlinear pseudo mobility (right). A grid cell is about 20 m in the z-direction, so the height of CO$_2$ in the must be over 20 m to give saturation 0.9 (1-S$_{rw}$) in the top cell.*
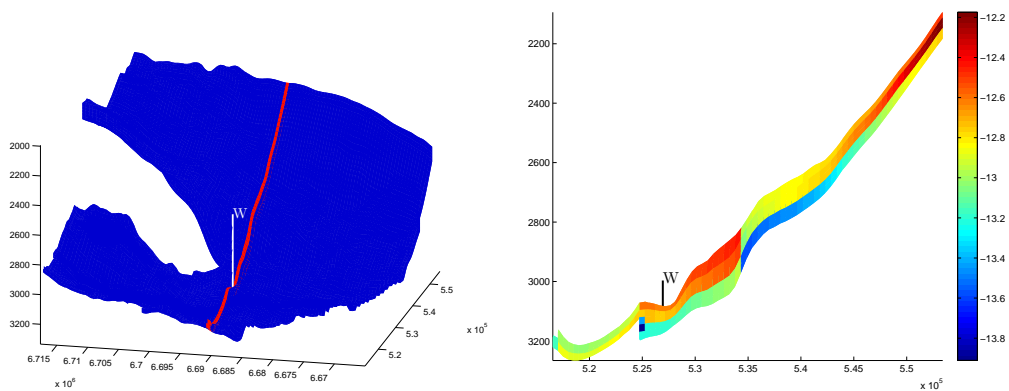
Figure 10 *Left: Well placement and direction of the 2D cut shown to the right with logarithm of permeability in the x-direction.*

Table 1 *Time steps [years] of different terms for the VE model.*

Time	Advection	Convection	Segregation	Parabolic
25	1	201	8	6
75	1	234	8	3
125	-	251	8	4
250	-	190	8	4
500	-	164	8	3

Table 2 *Time steps [years] of different terms for the 3D model.*

Time	Advection	Convection	Segregation
25	0.1	10	0.04
75	0.1	6	0.04
125	-	10	0.04
250	-	11	0.04
500	-	12	0.04

the saturation profiles seen in Figure 9.

The same simulations were run comparing averaged porosity and integrated porosity (Eq. 4). However, as could be expected, the differences between the two methods was not significant since the porosity variations are much smaller than the permeability variations.

Discussion of numerical methods

For the 3D calculations in this paper we used the MATLAB Reservoir Simulation Toolbox (MRST) (Lie et al., 2010; MRST), which at the present stage is based on a sequential splitting strategy. It contains a set of mimetic (Brezzi et al., 2005) and multiscale flow solvers and simple transport solvers capable of handling general unstructured, polyhedral grids. In this particular problem we used a mimetic pressure solver and a single point upwind transport solver. For the vertical equilibrium formulation we used a very similar approach, with mimetic discretization for the pressure equation. The transport equation was solved using a mobility upwind discretization where the parabolic term was treated explicitly for most of the cases. We also tested a semi-implicit approach where the parabolic term was solved implicitly. In the simulation we see that large errors can occur in the 3D simulation where a sharp interface approximation is valid. The error is caused by replacing the average of a function $F(S)$ by $F(\widetilde{S})$, where $\widetilde{S}$ denote the average of S in a cell. In our case it is particularly the averages of $f(S)$ in the transport equation and $f(S)\rho_{co2} + (1 - f(S))\rho_w$ in the pressure equation which cause the error.

In the post injection phase, the calculation is particularly vulnerable to this type of error since the only driving force is the interface-tilt in the interface compared to the gravity direction. If capillary forces would be considered, the same kind of error would occur when using grid cells of larger vertical size than the capillary fringe. For real field applications, the scale of the capillary fringe could vary from cm to m depending on the CO_2 capillary functions (Plug and Bruining, 2007). Whereas for the VE simulation, the accuracy is rather dependent on the possibility of neglecting vertical velocity. The VE assumption is valid if the quantity $\omega = K_x/K_z(\nabla h)^2 << 1$ (Bear, 1988). Figure 8 shows that this is the case for the Johansen formation except for a small area near the injection well.

For a discussion of the choice of numerical methods for simulation of CO_2 injection for large seques- tration projects, it is useful to estimate the time-step associated with the Courant–Friedrich–Lewi (CFL)

condition for the different terms involved. The time steps for the 3D simulation is for the segregation

$$t^{seg} \sim \Delta z / \left(K_z g \Delta \rho \frac{d}{dS} [\lambda_o f_w] \phi \right). \tag{10}$$

The convection step is determined by the gravity driven total velocity and thus depends on the particular distribution of the fluid. However, a useful estimate can be derived based on the VE equation. Assuming a thin CO_2 layer of height h, the CFL time step due to motion parallel to the surface, where x is the coordinate on the surface, is

$$t^{conv,x} \sim \Delta x / \left(K_x g f'(S) \frac{\Delta \rho}{\mu} (\mathbf{g}_\parallel(\mathbf{x}) - g_z(\mathbf{x}) \nabla p_c(S, \mathbf{x})) \phi \right). \tag{11}$$

For the VE formulation we would have the same time step restriction except for the term $f'(S)$, which is considered to be $1/(1 - S_{rw})$. The ratio of the segregation time step to the convection time step is

$$t^{seg}/t^{conv,x} \sim K_x \Delta z \frac{\partial h}{\partial x} / \left(K_z \Delta x \frac{d}{dS} [\lambda_o f_w] \mu \right). \tag{12}$$

The CLF conditions for the advection and the parabolic part of the VE model can be computed similarly. Using the above expressions we estimate the time steps in the numerical simulations, and the result is shown in Table 2 and Table 1. The fastest dynamics is identified as the segregation in the 3D model. For realistic simulation, we need methods that capture the stationary state of this dynamic well. An other clear observation is that the dominating time step restriction for the post injection period is the time steps needed to capture the segregation term in the VE formulation. This is expected since the fastest dynamics in this period corresponds to CO_2 flowing along the steepest surfaces. The convection velocity of the vertical equilibrium formulation is very small. This has the implication that a larger pressure-transport splitting step can be used with a vertical equilibrium model than with the 3D model. As long as the plume is not very step, i.e. just after the injection period is ended, a good approximation can be done by neglecting this term.

The model for Johansen used herein is a rather coarse mesh with lateral grid distances of about 400 m. In this case an explicit treatment of the parabolic term is appropriate. Since the time step restrictions of the parabolic term scales as $1/dx^2$ where dx is lateral grid size, we applied a semi-implicit method in this case, but for future work an operator splitting approach (Brusdal et al., 1997; Karlsen and Risebro, 1997) is needed. We will expect such approaches to be preferable for grid resolutions of about 50 m. A simple estimate shows that for the VE model, the numerical diffusion is larger than the physical diffusion if $h/dx < sin(\theta)$ in the post injection period, where θ is the angle of tilt of the top surface.

Since Eq. 7 has no self sharping mechanism for the parabolic term, care has to be taken for the solution not to be dominated by numerical diffusion. For the cases where explicit transport is possible, advances in using GPUs have shown large speed up over CPU implementations for hyperbolic equations (Brodtkorb et al., 2010; de la Asuncin M. et al., 2010). We believe that future work in this direction will give the possibility of large scale desktop simulation of VE models on coarse grids. In such a work, accurate discretization of the hyperbolic term will be essential.

Conclusions

We have investigated the advantages and disadvantages of using 3D and VE models for simulating CO_2 sequestration for a realistic storage aquifer. In particular, we point out that for grids with low z-resolution, a VE model is more accurate than a 3D model away from the well when the capillary effects are small. Moreover, the large timescale difference between the lateral and vertical movement of a CO_2 plume makes 3D numerical resolution of vertical dynamics intractable for the post injection period. This has been clearly demonstrated with the CFL time step restriction of the segregation step.

For the injection period, the assumption of the VE model is not fulfilled in the whole domain. This introduces some errors near the well, but for the coarse and rather homogeneous model we investigated

in this paper this has little influence on the final CO_2 distribution. For a more heterogeneous model, near well-modeling with the VE assumption has to be done with care or by using a 3D simulator. Further, we have also shown that it is important to preserve the 3D properties of the permeability field in the vertical equilibrium formulation.

Lastly, we point out that there is a stronger decoupling between the pressure and transport equations in the post injection scenario for the VE model compared with the 3D model. We believe that this feature could be utilized to develop fast simulation methods for large scale CO_2 migration problems.

References

Bear, J. [1988] *Dynamics of Fluids in Porous Media*. Dover, ISBN 0-486-45355-3.

Bergmo, P., Lindeberg, E., Riis, F. and Johansen, W.T. [2009] Exploring geological storage sites for CO2 from Norwegian gas power plants: Johansen formation. *Energy Procedia*, **1**(1), 2945 – 2952, ISSN 1876-6102, doi:10.1016/j.egypro.2009.02.070.

Brezzi, F., Lipnikov, K. and Simoncini, V. [2005] A family of mimetic finite difference methods on polygonial and polyhedral meshes. *Math. Models Methods Appl. Sci.*, **15**, 1533–1553, doi:10.1142/S0218202505000832.

Brodtkorb, A., Hagen, T.R., Lie, K.A. and Natvig, J.R. [2010] Simulation and visualization of the Saint-Venant system using GPUs. *Computing and Visualization in Science*, [forthcoming].

Brusdal, H.K., Karlsen, K.H., Brusdal, K., Dahle, H.K., Evje, S. and a. Lie, K. [1997] The corrected operator splitting approach applied to a nonlinear advection-diffusion problem. *Comput. Methods Appl. Mech. Engrg*, 167–3.

Celia, M.A., Bachu, S., Nordbotten, J.M., Kavetski, D. and Gasda, S. [2006] A risk assessment tool to quantify CO2 leakage potential through wells in mature sedimentary basins. *Proceedings of the 8th Conference on Greenhouse Gas Technologies*.

Class, H. et al. [2009] A benchmark study on problems related to CO2 storage in geologic formations. *Comp. Geosci.*, **13**(4), 409–434, doi:10.1007/s10596-009-9146-x.

Coats, K.H., Dempsey, J.R. and Henderson, J.H. [1971] The use of vertical equilibrium in two-dimensional simulation of three-dimensional reservoir preformance. *Soc. Pet. Eng. J.*, **Mar**, 68–71.

Coats, K.H., Nielsen, R.L., Terune, M.H. and G.Weber, A. [1967] Simulation of three-dimensional, two-phase flow in oil and gas reservoirs. *Soc. Pet. Eng. J.*, **Dec**, 377–388.

Dahle, H.K., Eigestad, G.T., Nordbotten, J.M. and Pruess, K. [2009] A model-oriented benchmark problem for CO2 storage. *http://org.uib.no/cipr/Workshop/2009/CO2/benchmark_definition.pdf*.

de la Asuncin M., Mantas, J.M. and Castro, M.J. [2010] Simulation of one-layer shallow water systems on multi-core and CUDA architectures. *Journal of Supercomputing*, **[In press]**.

Eigestad, G. et al. [2008] Geological and fluid data for modelling CO2 injection in the Johansen formation. Http://www.sintef.no/Projectweb/MatMorA/Downloads/Johansen.

Eigestad, G., Dahle, H., Hellevang, B., Riis, F., Johansen, W. and Øian, E. [2009] Geological modeling and simulation of CO2 injection in the Johansen formation. *Computational Geosciences*, **13**(4), 435–450, ISSN 1420-0597, doi:10.1007/s10596-009-9153-y.

Gasda, S.E., Nordbotten, J.M. and Celia, M.A. [2009] Vertical equilibrium with sub-scale analytical methods for geological C02 sequestration. *Special issue of Computational Geosciences*, **13**(4), 469–481, doi: 10.1007/s10596-009-9138-x.

Godderij, R., Bruining, J. and Molenaar, J. [1999] A fast 3D interface simulator for steamdrives. *SPE*, **4**(4), 400–408.

Hesse, M.A., Orr, F.M. and Tchelepi, H.A. [2008] Gravity currents with residual trapping. *J. Fluid. Mech.*, **611**, 35–60.

Hesse, M.A., Tchelepi, H.A., Cantwell, B.J. and Orr, F.M. [2007] Gravity currents in horizontal porous layers: transition from early to late self-similarity. *J. Fluid. Mech.*, **577**, 363–383.

Huppert, H.E. and Woods, A.E. [1995] Gravity-driven flows in porous layers. *J. Fluid Mech.*, **292**, 55–69.

Karlsen, K.H. and Risebro, N.H. [1997] Corrected operator splitting for nonlinear parabolic equations. *SIAM J. Numer. Anal*, **37**.

Lie, K.A., Krogstad, S., Ligaarden, I.S., Natvig, J.R., Nilsen, H.M. and Skaflestad, B. [2010] Discretisation on complex grids – open source MATLAB implementation. *Proceedings of ECMOR XII–12th European Conference on the Mathematics of Oil Recovery*, EAGE, Oxford, UK.

Lingli, W. and Fredrik, S. [2009] Estimate CO2 storage capacity of the Johansen formation: numerical investigations beyond the benchmarking exercise. *Computational geoscience*, **13**, 451–461.

Lyle, S., Huppert, H.E., Hallworth, M., Bickle, M. and Chadwick, A. [2005] Axisymmetric gravity currents in a porous media. *J. Fluid. Mech.*, **543**, 293–302, doi:10.1017/S0022112005006713.

MacMinn, C.W. and Juanes, R. [2009] Post-injection spreading and trapping of CO2 in saline aquifers: Impact of the plume shape at the end of injection. *Comp. Geosci.*, **13**, 483–491.

Martin, J.C. [1958] Some mathematical aspects of two phase flow with application to flooding and gravity segregation. *Prod. Monthly*, **22**(6), 22–35.

Martin, J.C. [1968] Partial integration of equation of multiphase flow. *Soc. Pet. Eng. J.*, **Dec**, 370–380.

Metz, B., Davidson, O., de Coninck, H., Loos, M. and Meyer, L. [2005] *Special Report on Carbon Capture and Storage*. Cambridge University Press, UK.

MRST [2009] MATLAB Reservoir Simulation Toolbox, http://www.sintef.no/mrst/.

Neuman, C. [1985] A gravity override model of steamdrive. *JPT*, **37**(1), 163–189.

Nordbotten, J.M. and Celia, M.A. [2006] Analysis of plume extent using analytical solutions for CO2 storage. *Proceedings of the 16th conference on Computational Methods in Water Resources*.

Nordbotten, J., Celia, M. and Bachu, S. [2005] Analytical solution for CO2 plume evolution during injection. *Transp. Porous Media*, **58**(3), 339–360.

Plug, W.J. and Bruining, J. [2007] Capillary pressure for the sand-CO2-water system under various pressure conditions. application to CO2 sequestration. *Advances in Water Resources*, **30**(11), 2339 – 2353, ISSN 0309-1708, doi:DOI: 10.1016/j.advwatres.2007.05.010.

Vella, D. and Huppert, H.E. [1995] Gravity currents in a pourous medium at an inclinded plane. *Journal of Fluid Mechanics*, **292**, 59–65.